Journal of Power Sources 219 (2012) 249–252

Contents lists available at SciVerse ScienceDirect

Journal of Power Sources

journal homepage: www.elsevier.com/locate/jpowsour

Short communication

A novel non-precious metal catalyst synthesized via pyrolysis of polyaniline-coated tungsten carbide particles for oxygen reduction reaction

Kezhu Jiang, Qingmin Jia, Mingli Xu, Daping Wu, Lunquan Yang, Guotao Yang, Linyan Chen, Guanghua Wang, Xikun Yang*

Research Center for Analysis and Measurement, Kunming University of Science and Technology, Kunming 650093, PR China

HIGHLIGHTS

- We develop a novel W–N–C catalyst for ORR.
- The W–N–C catalyst exhibits an excellent ORR activity in acidic media.
- The presence of W species contributes to growth of nanoshell structure.
- This work offers a new route to designing and developing new kinds of NPMCs.

GRAPHICAL ABSTRACT

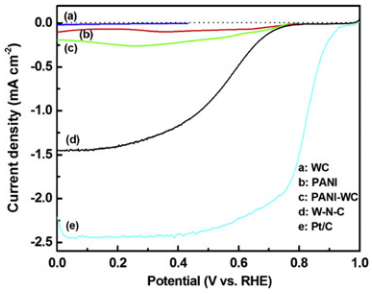

ARTICLE INFO

Article history:
Received 23 June 2012
Received in revised form
17 July 2012
Accepted 19 July 2012
Available online 2 August 2012

Keywords:
Non-precious metal catalysts
Pyrolysis
Nanoshell structure
Oxygen reduction reaction

ABSTRACT

In this paper, a novel non-precious metal catalyst, W–N–C, for oxygen reduction reaction (ORR), has been synthesized via the pyrolysis of polyaniline-coated tungsten carbide particles. The electrocatalytic measurements show that the W–N–C catalyst exhibits a high catalytic activity and long-term stability for ORR in acid media. The ORR onset potential, half-wave potential, and diffusion-limited current density of W–N–C catalyst are measured at 0.82 V, 0.55 V, and 1.54 mA cm^{-2}, respectively. TEM and XPS measurements indicate that the W–N–C catalyst has nanoshell structure and a high ratio of the graphitic N, which are responsible for high ORR activity and stability.

1. Introduction

With the high efficiency, low temperature of operation, and zero emission, the proton exchange membrane fuel cells (PEMFCs) have been considered as one of the most promising energy conversion technologies. It is well known that platinum is still regarded as an ideal cathode in PEMFCs for its excellent catalytic activity for ORR. However, the issues of limited resources, high price and low tolerance to CO poisoning limit Pt cathode application [1,2]. In order to decrease the cost of catalysts and eliminate their dependence on precious metal, developing non-precious metal catalysts (NPMCs) is essential for the commercialization of PEMFCs technology.

Up to date, several types of NPMCs such as Fe/N/C or Co/N/C catalysts [3,4], conductive polymers [5,6], transition metal chalcogenides [7,8], metal carbides and nitrides [9,10] have been demonstrated as catalysts for ORR. Compared with other NPMCs, conductive polymers such as polyaniline (PANI), polypyrrole, and

* Corresponding author. Tel.: +86 871 5110975; fax: +86 871 5111617.
E-mail address: yxk630@hotmail.com (X. Yang).

0378-7753/$ – see front matter © 2012 Elsevier B.V. All rights reserved.
http://dx.doi.org/10.1016/j.jpowsour.2012.07.056

polythiophen have attracted great interest due to their low cost, high electronic conductivity and distinct redox properties for ORR [11,12]. Especially, much attention has been paid to the PANI because of its facile synthesis, environmental stability, and simple doping/dedoping chemistry [13]. On one hand, PANI as a precursor material for Fe/N/C or Co/N/C catalysts displays very promising ORR activity and stability [14], but PANI alone has low ORR activity [6]. On the other hand, tungsten carbide (WC) has been used as a catalyst because of its platinum-like electron structure, stability in acidic solutions, and resistance to CO poisoning [15,16]. However, utilizing WC as a catalyst for ORR also has poor catalytic activity [9]. To the best of our knowledge, there have been no attempts so far to utilize a hybrid material of PANI and WC as a catalyst for ORR.

In this work, W–N–C catalyst for ORR was synthesized via the pyrolysis of PANI-coated WC particles. While PANI or WC alone has poor catalytic activity, their hybrid exhibits an excellent catalytic activity toward ORR after pyrolysis. This work offers a new route to designing and developing new kinds of NPMCs for ORR.

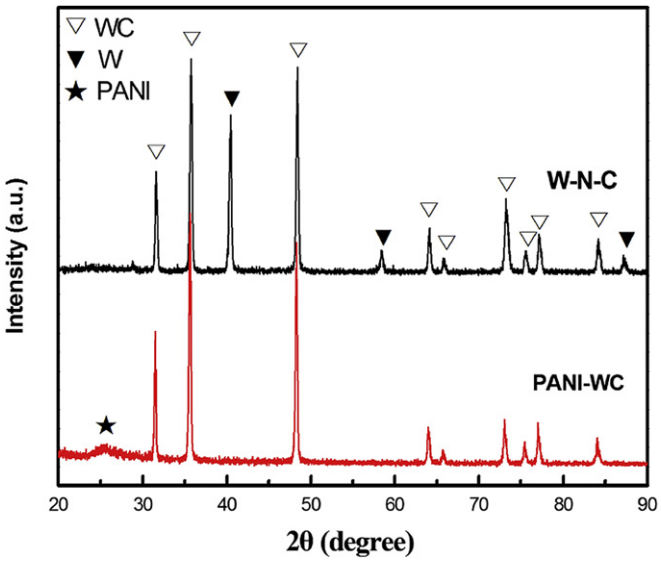

Fig. 2. XRD patterns of W–N–C and PANI–WC.

2. Experimental

2.1. Synthesis of catalysts

The PANI-coated WC particles were synthesized by in-situ polymerization method. WC (1 μm diameter) was treated in H_2SO_4 solution for 12 h 4.0 mL aniline was first dispersed with 0.9 g acid-treated WC in 0.5 M H_2SO_4 solution. The suspension was kept below 10 °C while the oxidant (ammonium peroxydisulfate) was added. After constant mixing for 12 h to allow the polymerized PANI to uniformly mix and coat the WC particles, the suspension was washed and filtrated by 0.5 M H_2SO_4 solution and deionized water. The obtained solid product was denoted as PANI–WC. Then, PANI–WC was pyrolyzed at 1000 °C in nitrogen gas for 1 h. The final sample was denoted as W–N–C.

2.2. Physical and electrochemical characterizations

Samples morphology was analyzed by transmission electron microscopy (TEM) using a JEM 2100 instrument at 200 kV. The crystal structure of the samples were identified by X-ray diffraction (XRD) using a Bruker D8 Advance X-ray diffractometer with Cu Kα (0.15406 nm) radiation. X-ray photoelectron spectroscopy (XPS) experiments were performed with a PHI5500 spectrometer using Mg Kα (1253.6 eV) radiation. Spectral correction was based on adventitious carbon, using the C1s binding energy of 284.8 eV.

Rotating disk electrode (RDE) voltammetry was tested in a conventional three-electrode system. A platinum wire and a Ag/AgCl electrode were used as the counter and reference electrode,

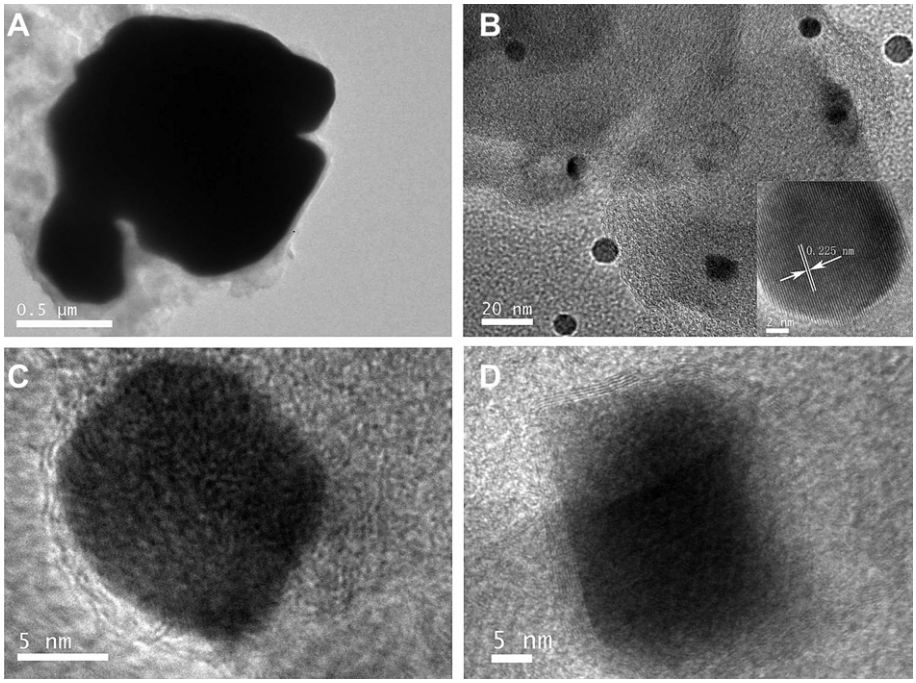

Fig. 1. TEM images of W–N–C: (A) WC particle; (B) W nanoparticles and inset: HR-TEM image of W nanoparticle; (C) W nanoparticle coated by carbon layer of amorphous microstructures; (D) W nanoparticle coated by well-aligned graphitic layers.

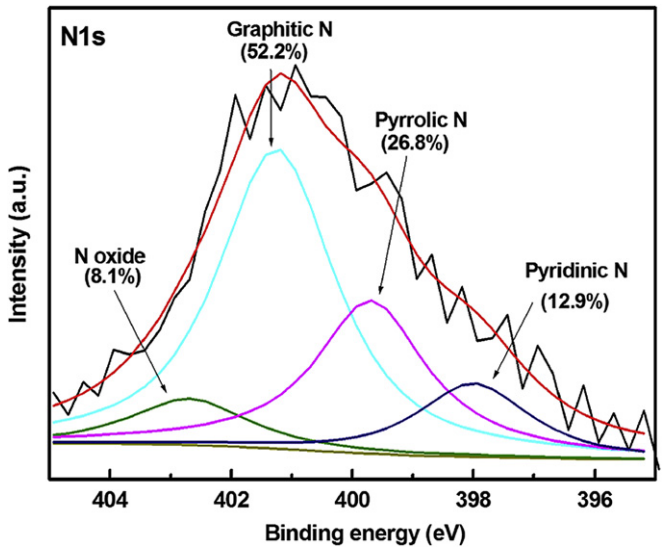

Fig. 3. XPS spectrum of N1s region for W–N–C.

respectively. All potentials here were transferred to refer to the reversible hydrogen electrode (RHE). The catalyst ink was prepared by ultrasonically mixing 6 mg of PANI–WC with 950 μL of isopropyl alcohol and 50 μL of 5 wt.% Nafion solution for 30 min. 10 μL of the suspension was deposited onto a polished tip of a glassy carbon disk (4.0 mm diameter and 0.48 mg cm^{-2} catalyst loading) and dried at room temperature. All electrochemical measurements were performed at room temperature in the RDE electrochemical cell and 0.5 M H_2SO_4 solution as electrolyte. The ORR current was determined by subtracting the N_2 current from the O_2 current. For comparison, a commercially available Pt/C catalyst (20 wt.% Pt, Johnson–Matthey) was used under the same conditions.

3. Results and discussion

3.1. Physical characterizations of the W–N–C catalyst

TEM images of W–N–C catalyst are shown in Fig. 1. In Fig. 1A, it can be seen that WC particles are covered by a carbon layer. As shown in Fig. 1B, the particles are dispersed on carbon surface and the average size of the particles is about 10 nm. The HR-TEM image of Fig. 1B shows that the lattice parameter of nanoparticle is 0.224 nm, which corresponds to the W (110) plane. Fig. 1C shows that W nanoparticle is coated by carbon layer of amorphous microstructures, while Fig. 1D shows that W nanoparticle is coated by well-aligned graphitic layers. In previous studies, metal species, such as Fe, Co and Ni, are often employed as catalysts for the controlled formation of various forms of carbon nanostructures [17–21]. However, from the above observations, we also observe the nanoshell morphology in the W–N–C catalyst. This suggests that the presence of W species contributes to growth of nanoshell structure of W–N–C catalyst during pyrolysis process.

XRD patterns of W–N–C and PANI–WC are presented in Fig. 2. Obviously, the samples contain different phase structures. The patterns of two samples show the typical diffraction peaks of WC phase (JCPDS No. 25-1047). Moreover, a small peak is also found at about 25.2° in the pattern of PANI–WC, which can be attributed to PANI [22]. However, this peak disappears in the pattern of W–N–C, which suggests that the PANI is decomposed after pyrolysis. The diffraction peaks of W–N–C located at 40.2°, 58.3° and 87.0° in the

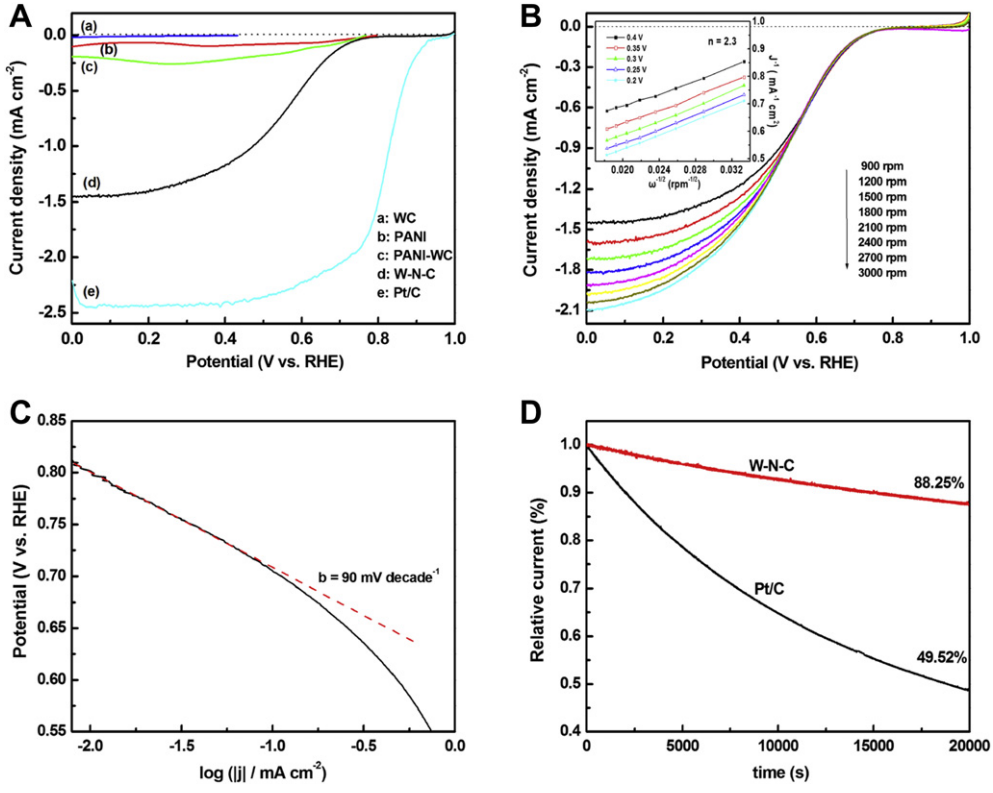

Fig. 4. (A) The ORR polarization curves of WC, PANI, PANI–WC and W–N–C in oxygen-saturated 0.5 M H_2SO_4 solution at 5 mV s^{-1} and 900 rpm. (B) The ORR polarization curves of W–N–C at various rotating speeds. Inset is the corresponding Koutecky–Levich plots. (C) Tafel slope of W–N–C derived by the mass-transport correction of corresponding RDE data (see Fig. 4A). (D) Current–time (i–t) chronoamperometric responses of W–N–C and Pt/C in oxygen-saturated 0.5 M H_2SO_4 solution at 5 mV s^{-1} and 900 rpm.

patterns can be attributed to crystalline W (JCPDS No. 4-806), which indicates that WC phase partially transforms into W phase after pyrolysis.

Fig. 3 shows the XPS spectrum of N1s region for W–N–C catalyst. The N/C atomic ratio is 1.9 at.% at the surface of W–N–C catalyst. The N1s spectra can be deconvoluted into four peaks, which are assigned to N oxide (402.7 eV, 8.1 at.%), graphitic N (401.2 eV, 52.2 at.%), pyrrolic N (399.8 eV, 26.8 at.%) and pyridinic N (398.1 eV, 12.9 at.%) [23,24]. From the deconvolution results, it is clear that the W–N–C catalyst shows a high ratio of graphitic N (52.2%).

3.2. Electrochemical characterizations of the W–N–C catalyst

The ORR polarization curves of WC, PANI, PANI–WC, W–N–C and Pt/C are shown in Fig. 4A. It is shown that PANI, WC and PANI–WC have a poor ORR activity, while W–N–C catalyst exhibits surprisingly high ORR activity in acid media. However, it can also be seen that the W–N–C catalyst shows a lower performance than that of Pt/C. The ORR onset potential, half-wave potential, and diffusion-limited current density of this catalyst are 0.82 V, 0.55 V, and 1.54 mA cm^{-2}, respectively. The high ORR activity can be attributed to the presence of nanoshell structure [19,21] and a high ratio of graphitic N [25,26] in the W–N–C catalyst. Fig. 4B shows the ORR polarization curves of W–N–C catalyst obtained at rotating rate range from 900 to 3000 rpm. Typically, the reaction seems to be under a combined kinetic-diffusion control of charge transfer and mass transport. It is shown that the electrode rotation has an effect on the reaction rate at lower potentials for ORR. According to the Koutecky–Levich equation and plots (the inset of Fig. 4B) [27], the electron number involved in the W–N–C catalyst for ORR is 2.3. This suggests that most of the molecular oxygen is reduced to H_2O_2 via a two-electron process. The Tafel slope of W–N–C catalyst derived by the mass-transport correction of corresponding RDE data (see Fig. 4A) is shown in Fig. 4C. The Tafel slop obtained toward the ORR is 90 mV $decade^{-1}$. The durabilities of the W–N–C and Pt/C catalysts were compared in Fig. 4D. The catalysts were held at 0.4 V for 20,000 s in oxygen-saturated 0.5 M H_2SO_4 solution at 5 mV s^{-1} and 900 rpm. From the Fig. 4D, the W–N–C has a superior durability compared to the Pt/C catalyst, which can be attributed to the high ratio of graphitic N of W–N–C catalyst [28]. The above results suggest that the W–N–C catalyst exhibits a high catalytic activity and stability for ORR in acid media. Further optimization of preparative parameters of the W–N–C catalyst is under way. It is expected that the performance of the catalyst could be further improved.

4. Conclusions

A novel W–N–C catalyst for ORR was successfully synthesized by the pyrolysis of PANI-coated WC particles. The electrocatalytic performances demonstrated that PANI or WC alone has poor catalytic activity, while W–N–C catalyst exhibits an excellent catalytic activity for ORR. The W–N–C catalyst catalyzed ORR is a two-electron process. This W–N–C catalyst shows a promising application in PEMFCs. This work essentially offers a new approach to development of NPMCs for ORR.

Acknowledgments

This work was supported by the National Natural Science Foundation of China (Projects 20863003 and 51164017) and the Yunnan Province (Projects 2007PY01-9 and 2010DH025).

References

[1] F. Jaouen, E. Proietti, M. Lefevre, R. Chenitz, J.P. Dodelet, G. Wu, H.T. Chung, C.M. Johnston, P. Zelenay, Energy & Environmental Science 4 (2011) 114–130.
[2] M. Winter, R.J. Brodd, Chemical Reviews 104 (2004) 4245–4269.
[3] R. Jasinski, Nature 201 (1964) 1212–1213.
[4] M. Lefevre, E. Proietti, F. Jaouen, J.-P. Dodelet, Science 324 (2009) 71–74.
[5] G. Wu, Z.W. Chen, K. Artyushkova, F.H. Garzon, P. Zelenay, ECS Transactions 16 (2008) 159–170.
[6] V.G. Khomenko, V.Z. Barsukov, A.S. Katashinskii, Electrochimica Acta 50 (2005) 1675–1683.
[7] N.A. Vante, H. Tributsch, Nature 323 (1986) 431–432.
[8] K. Lee, L. Zhang, J. Zhang, Journal of Power Sources 165 (2007) 108–113.
[9] K. Lee, A. Ishihara, S. Mitsushima, N. Kamiya, K.-i. Ota, Electrochimica Acta 49 (2004) 3479–3485.
[10] H. Zhong, H. Zhang, Y. Liang, J. Zhang, M. Wang, X. Wang, Journal of Power Sources 164 (2007) 572–577.
[11] W.M. Millan, T.T. Thompson, L.G. Arriaga, M.A. Smit, International Journal of Hydrogen Energy 34 (2009) 694–702.
[12] U. Rammelt, P.T. Nguyen, W. Plieth, Electrochimica Acta 48 (2003) 1257–1262.
[13] E. Antolini, E.R. Gonzalez, Applied Catalysis A: General 365 (2009) 1–19.
[14] G. Wu, K.L. More, C.M. Johnston, P. Zelenay, Science 332 (2011) 443–447.
[15] L.H. Bennett, J.R. Cuthill, A.J. McAlister, N.E. Erickson, R.E. Watson, Science (New York, N.Y.) 184 (1974) 563–565.
[16] J.B. Christian, S.P.E. Smith, M.S. Whittingham, H.D. Abruna, Electrochemistry Communications 9 (2007) 2128–2132.
[17] N.M. Rodriguez, Journal of Materials Research 8 (1993) 3233–3250.
[18] R.T.K. Baker, Carbon 27 (1989) 315–323.
[19] P.H. Matter, L. Zhang, U.S. Ozkan, Journal of Catalysis 239 (2006) 83–96.
[20] Y. Nabae, S. Moriya, K. Matsubayashi, S.M. Lyth, M. Malon, L. Wu, N.M. Islam, Y. Koshigoe, S. Kuroki, M.-a. Kakimoto, S. Miyata, J.-i. Ozaki, Carbon 48 (2010) 2613–2624.
[21] J.-i. Ozaki, S.-i. Tanifuji, A. Furuichi, K. Yabutsuka, Electrochimica Acta 55 (2010) 1864–1871.
[22] J. Yan, T. Wei, Z. Fan, W. Qian, M. Zhang, X. Shen, F. Wei, Journal of Power Sources 195 (2010) 3041–3045.
[23] J.R. Pels, F. Kapteijn, J.A. Moulijn, Q. Zhu, K.M. Thomas, Carbon 33 (1995) 1641–1653.
[24] Z.R. Ismagilov, A.E. Shalagina, O.Y. Podyacheva, A.V. Ischenko, L.S. Kibis, A.I. Boronin, Y.A. Chesalov, D.I. Kochubey, A.I. Romanenko, O.B. Anikeeva, T.I. Buryakov, E.N. Tkachev, Carbon 47 (2009) 1922–1929.
[25] H. Niwa, M. Kobayashi, K. Horiba, Y. Harada, M. Oshima, K. Terakura, T. Ikeda, Y. Koshigoe, J.-i. Ozaki, S. Miyata, S. Ueda, Y. Yamashita, H. Yoshikawa, K. Kobayashi, Journal of Power Sources 196 (2011) 1006–1011.
[26] X. Wang, Z. Hou, T. Ikeda, S.-F. Huang, K. Terakura, M. Boero, M. Oshima, M.-a. Kakimoto, S. Miyata, Physical Review B 84 (2011).
[27] M.S. El-Deab, T. Ohsaka, Electrochimica Acta 47 (2002) 4255–4261.
[28] G. Liu, X. Li, P. Ganesan, B.N. Popov, Electrochimica Acta 55 (2010) 2853–2858.